Green Chemistry

Cite this: *Green Chem.*, 2012, **14**, 3220

www.rsc.org/greenchem

PAPER

Direct amide bond formation from carboxylic acids and amines using activated alumina balls as a new, convenient, clean, reusable and low cost heterogeneous catalyst†

Sabari Ghosh,[a] Asim Bhaumik,[b] John Mondal,[b] Amit Mallik,[c] Sumita Sengupta (Bandyopadhyay)[d] and Chhanda Mukhopadhyay*[a]

Received 9th June 2012, Accepted 13th September 2012
DOI: 10.1039/c2gc35880h

For the first time, we have used activated alumina balls (3–5 mm diameter) for amide synthesis from carboxylic acids (unactivated) and amines (unactivated) under neat reaction conditions that produce no toxic by-products and has the advantages of being low-cost, easily available, heterogeneous, reusable and environmentally benign with no troublesome/hazardous disposal of the catalyst.

Introduction

The amide bond plays a major role in the elaboration and composition of biological systems. It is one of the most important linkages in organic chemistry and constitutes the key functional group in peptides, polymers, many natural products and pharmaceuticals.[1] An in-depth analysis of the comprehensive medicinal chemistry database revealed that the carboxamide group appears in more than 25% of known drugs.[2] A recent report by the American Chemical Society Green Chemistry Institute Pharmaceutical Roundtable (ACS GCIPR) has found that amide formation, avoiding poor atom economy reagents, is the priority area of research for the pharmaceutical industry.[3a] Catalytic amide formation was recently highlighted as a reaction of importance from a 'green chemistry' perspective.[3b] As many as 65% of drug molecules prepared by leading pharmaceutical companies contain an amide unit, indicating its importance and prevalence in synthetic organic chemistry. The occurrence of an amide functionality, particularly in peptides and proteins, sometimes gives the incorrect impression that there are no remaining synthetic challenges. This is surprising, as it is often the case that even simple amides resist formation, forcing practitioners to resort to ever more exotic and expensive reagents for their synthesis. Furthermore, the favourable properties of amides, such as high polarity, stability and conformational diversity, make it one of the most popular and reliable functional groups in all branches of organic chemistry. Improved methods for the synthesis of an amide functionality, particularly waste-free and suitable for fragment coupling, are in great demand.

In general, traditional approaches for amide synthesis rely heavily on the use of activated carboxylic acids and amines, which often require stoichiometric amounts of coupling reagents and produce toxic chemical waste.[4,2a] Catalytic oxidative methods have become a powerful tool for the construction of amide complexes, in which oxygen atoms of amides generally originate from oxone/H_2O_2 [5] or oxygen-containing carbonyl precursors including aldehydes[6] and alcohols.[7] Such well developed oxidative reactions usually require stoichiometric oxidants such as TBHP[6a,b] and oxone,[5,6c] expensive or relatively complex transition metal catalysts such as Ru,[7a–c] Rh,[6d,7d] and Mn[5] complexes. Catalytic hydration of organonitriles was also researched extensively by Bera *et al.* and Tu *et al.*[8] An organometallic catalyst was developed that utilizes a ligand scaffold to engage in secondary interactions with water and thus facilitates the hydration of nitriles.[8a] Transition metal-free catalytic hydration of organonitriles to amides was also developed by Tu *et al.*[8b]

Direct uncatalyzed formation of amides has been observed as a background reaction in studies of catalytic amide formation. Cossy and Palegrosdemange (1989) reported the synthesis of a small range of amides at 140 °C under neat conditions in the presence of 4 Å molecular sieves[9] and a later report by Gooßen *et al.* showed a larger range of amides could be formed under solvent-free thermal conditions (160 °C), again in the presence of molecular sieves.[10] Whiting *et al.* (2006) observed 60% conversion into *N*-benzyl-4-phenylbutyramide after heating 4-phenylbutyric acid and benzylamine in toluene at reflux for 22 hours in the presence of 3 Å molecular sieves[11] and also published a detailed study into the reaction mechanism by which direct amide bond formation may occur in non-polar, aprotic solvents.[12] Clark *et al.* (2009) reported a heterogeneous silica catalyst for direct amidation in refluxing toluene.[13]

[a]*Department of Chemistry, University of Calcutta, 92 APC Road, Kolkata-700009, India. E-mail: cmukhop@yahoo.co.in; Tel: +91 9433019610*
[b]*Department of Materials Science, Indian Association for the Cultivation of Science, Jadavpur, Kolkata, 700 032, India*
[c]*Department of Chemical Technology, University of Calcutta, 92 APC Road, Kolkata-700009, India*
[d]*Department of Biophysics, Molecular Biology and Bioinformatics, University of Calcutta, 92 APC Road, Kolkata-700009, India*
†Electronic supplementary information (ESI) available. See DOI: 10.1039/c2gc35880h

Results and discussion

The present methodology, which utilizes cheap and easily available alumina balls (activated) as a heterogeneous catalyst, opens up a new and attractive window for the one-step synthesis of an amide functionality in a less hazardous metal-free methodology. From the environmental and economic point of view, a reaction with inexpensive heterogeneous catalyst is always desired. The direct condensation to form amides is highly desirable as both poor atom economy and step economy can be avoided, the only side product being water. Moreover, the use of alumina balls in assisting amide synthesis lead to a very clean reaction and the end of life prospects for the catalyst are attractive, as minimal preparation is required when disposal is eventually needed. This direct condensation also leads to easy procurement of the components. Herein, we demonstrate the first example of a heterogeneously catalyzed reaction of carboxylic acids with amines to form amides and H_2O using the easily available simple activated alumina ball catalyst.

Activated alumina balls (ESI Part 1, Fig. S1–S3†) is an aluminum oxide which is highly porous and exhibits a tremendous surface area. Activated alumina (balls) is resistant to thermal shock and abrasion and does not shrink, swell, soften or disintegrate during the reaction. The EDS X-ray spectrum of an alumina ball shows 46.90% by weight of oxygen and 53.10% by weight of aluminium (ESI Part 1, Table S1, Fig. S4†). With the aim of developing a new high activity *green* catalyst for a direct amidation reaction, we effectively carried out the synthesis with an alumina (balls) catalyst.

The reaction of 4-chloroaniline with heptanoic acid, as a model reaction, was examined under various catalytic conditions (Table 1). There was no reaction in the absence of a catalyst. Neutral alumina failed to give the desired product. Activated alumina balls very successfully catalysed the amide synthesis. Activation temperatures were investigated (Table 1) and calcination at 700 °C gave the highest yields (98%). A comparable activity was observed also at 400 °C calcination (95%). There is a sharp jump in the yield (Fig. 1) upon increasing the calcination temperature from 120 °C (73%) to 400 °C (95%). The calcination temperature was not increased over 700 °C since a nearly quantitative yield was obtained (98%). A very high catalyst loading was not required (only 10 wt% of the total mass of the reactants gave the highest yields, see Table 1) which is another advantage of this methodology. Removing water from the system was also not required. Reaction under an inert atmosphere did not enhance the yields. This is a solvent-free synthesis and therefore volatile solvents or procuring "dry" solvents were not required, thus simplifying the process. By-products were not observed and only unreacted acid and amine remained in trace amounts. The carbon balance of the reaction was 100% (% carbon in the reactants incorporated into the final product).

A maximum activity of calcinations at 700 °C can be attributed to the fact that the morphology of the alumina balls change upon calcination, with a sharp decrease in the BET surface area (Fig. 2). Although, this change in the structure of the alumina balls is not very prominent (Fig. S1 and S2,† ESI Part 1), the high resolution SEM images (Fig. 3) show that the shape changes from "spherical" to "rhombohedral" and the size of the aggregated particles increases upon calcination to 120 °C (average 710 nm aggregates), 400 °C (average 768 nm aggregates) and finally to 700 °C (average 794 nm aggregates). The change is very distinct at 700 °C. This change in shape leading to an increased particle aggregate size, in turn leading to a decreased BET surface area (Fig. 2), which leads to a nearly quantitative reaction yield, *i.e.*, 98% (Table 1), of compound heptanoic acid (4-chloro-phenyl)-amide (**3ik**, Table 2).

Table 1 Synthesis of heptanoic acid (4-chloro-phenyl)-amide

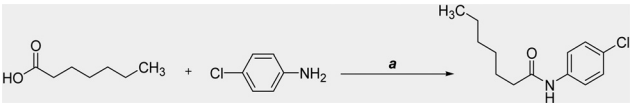

Catalyst	Calcination temperature (°C)	Catalyst loading (wt%)	Conversion[b] (%)
Neutral alumina	—	0	0
		10	0
		20	0
Neutral alumina	700	0	0
		10	0
		20	0
		50	0
Alumina balls[c]	—	0	0
		10	65
		50	65
Alumina balls[c]	120	5	50
		10	73
		20	73
		50	73
Alumina balls[c]	400	5	65
		10	95
		20	95
Alumina balls[c]	700	5	70
		10	98
		20	98
None	—	—	0

[a] 0–50 wt% of catalyst in relation to total mass of reagents (exact catalyst loading mentioned in column 3 of the table), neat reaction conditions at 140 °C for 3 hours, 10 mmol of Heptanoic acid and 10 mmol of 4-chloroaniline. [b] Isolated yield. [c] Activated alumina balls from Sorbead India.

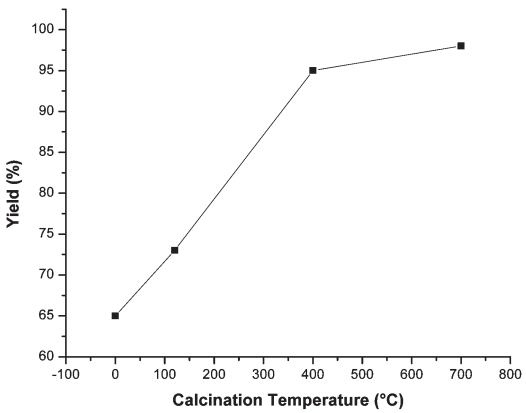

Fig. 1 Variation of isolated yield of heptanoic acid (4-chloro-phenyl)-amide (**3ik**, Table 2) with change in calcination temperature of the catalyst alumina balls.

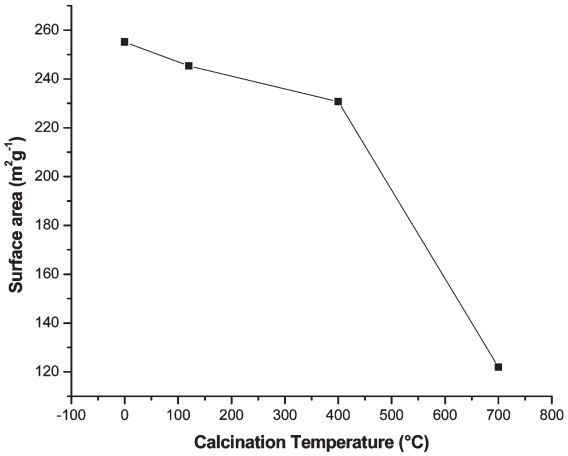

Fig. 2 Variation of the BET surface area of the alumina ball catalyst with the activation temperature.

Using the above optimized conditions, the scope of the activated alumina balls as catalyst was explored for the direct amidation of a variety of carboxylic acids and amines. The results are summarized in Table 3. The acids **p**, **g**, **q** and **n** were prepared by refluxing succinic anhydride (**5**) with pyrrolidine (**4a**), piperidine (**4b**), morpholine (**4c**) and *N*-methyl piperazine (**4d**) (Scheme 1). These sensitive functionalised acids were then reacted with the corresponding amines in the presence of activated alumina balls to form the amide (diamide in these cases) in compounds **3gh**, **3gj**, **3gm**, **3nl**, **3no**, **3gl**, **3go**, **3pl**, **3po**, **3ql** and **3qo** in considerable yields.

The catalyst displayed high activity for amidation of all combinations of aromatic and aliphatic carboxylic acids and amines. The reaction shows good results without any significant influence of the structure of the reactants on the product yields. A minimum of around 70% yield is reached in the cases studied. We propose the highly porous and aggregated particle nature of these activated alumina ball catalysts (see SEM images, Fig. 3 and the porosimetry data, graphs Table 3, Fig. 4–9) is responsible for such high yielding reactions. The SEM images (Fig. 3) indicate that the size of the aggregated particle increases with the increase in the activation temperature. This is reflected in the decrease of the BET surface area in that order (Table 3). A maximum activity of the sample on activation at 700 °C could be attributed to the fact that the morphology of the alumina ball changes upon calcination. The particle aggregates change shape from *spherical* to *rhombohedral* upon calcination to 700 °C. Further, the porosity measurement showed that the surface area of the material (by nitrogen adsorption at 77 K) decreases upon increasing of the activation temperature from 120 °C, 400 °C and 700 °C, and did not correlate directly with the catalyst activity. However, the pore volume (0.3635 ccg^{-1}) and pore width (10.8 nm) is maximum at the 700 °C activation temperature and these factors play the most important role. This high pore width and pore volume favors easy diffusion of the substrate and product molecules during the reaction. When the calcined alumina spheres adsorb the water and, as one of the products is removed from the reaction media, the reaction equilibrium is constantly shifted towards the formation of amide and thus higher yields are obtained. The surface area (88 m^2 g^{-1}) and pore volume (0.1675 ccg^{-1}) of neutral alumina is very low when compared to that of the alumina balls even at room-temperature

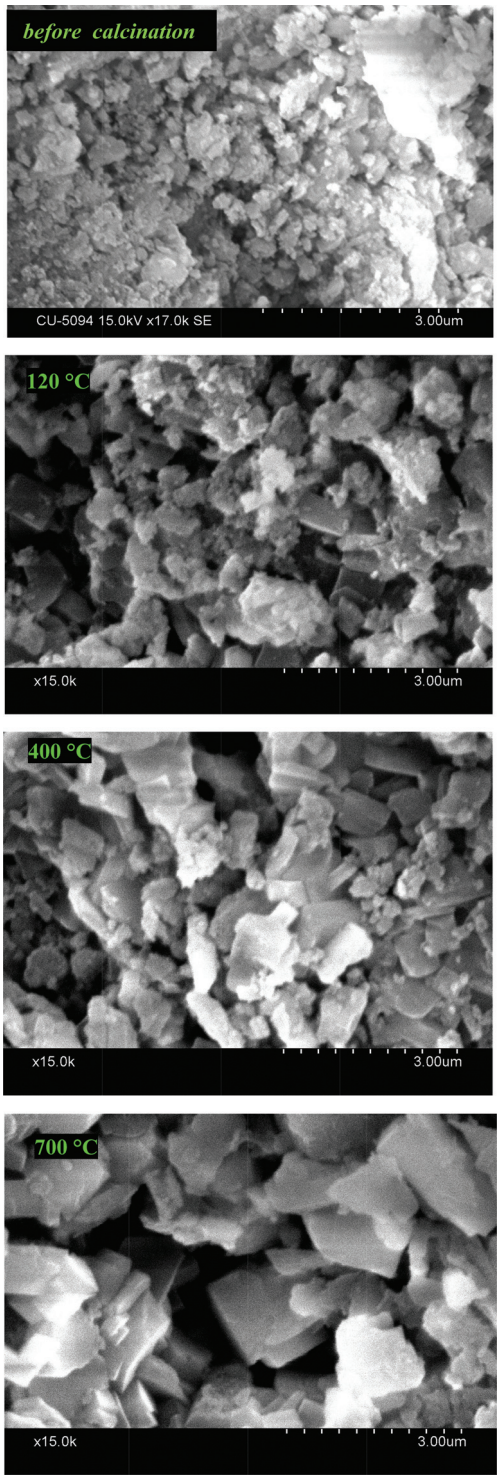

Fig. 3 From top: the close-up SEM images of an activated alumina ball before calcination (99–175 nm particle aggregates), after calcination at 120 °C, 400 °C and 700 °C. The particle aggregates change shape from *spherical* to *rhombohedral* upon calcination to 700 °C. The particle aggregate size (enlarged SEM images with the particular aggregate size given in ESI,† Part 1) also increases progressively upon calcination at 120 °C (614–818 nm aggregates), 400 °C (636–889 nm aggregates) and 700 °C (587–938 nm aggregates).

Table 2 Results for the reaction of direct amide bond synthesis[a,b]

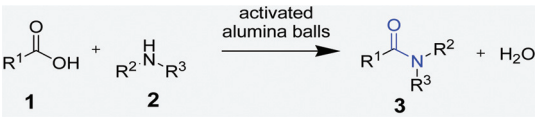

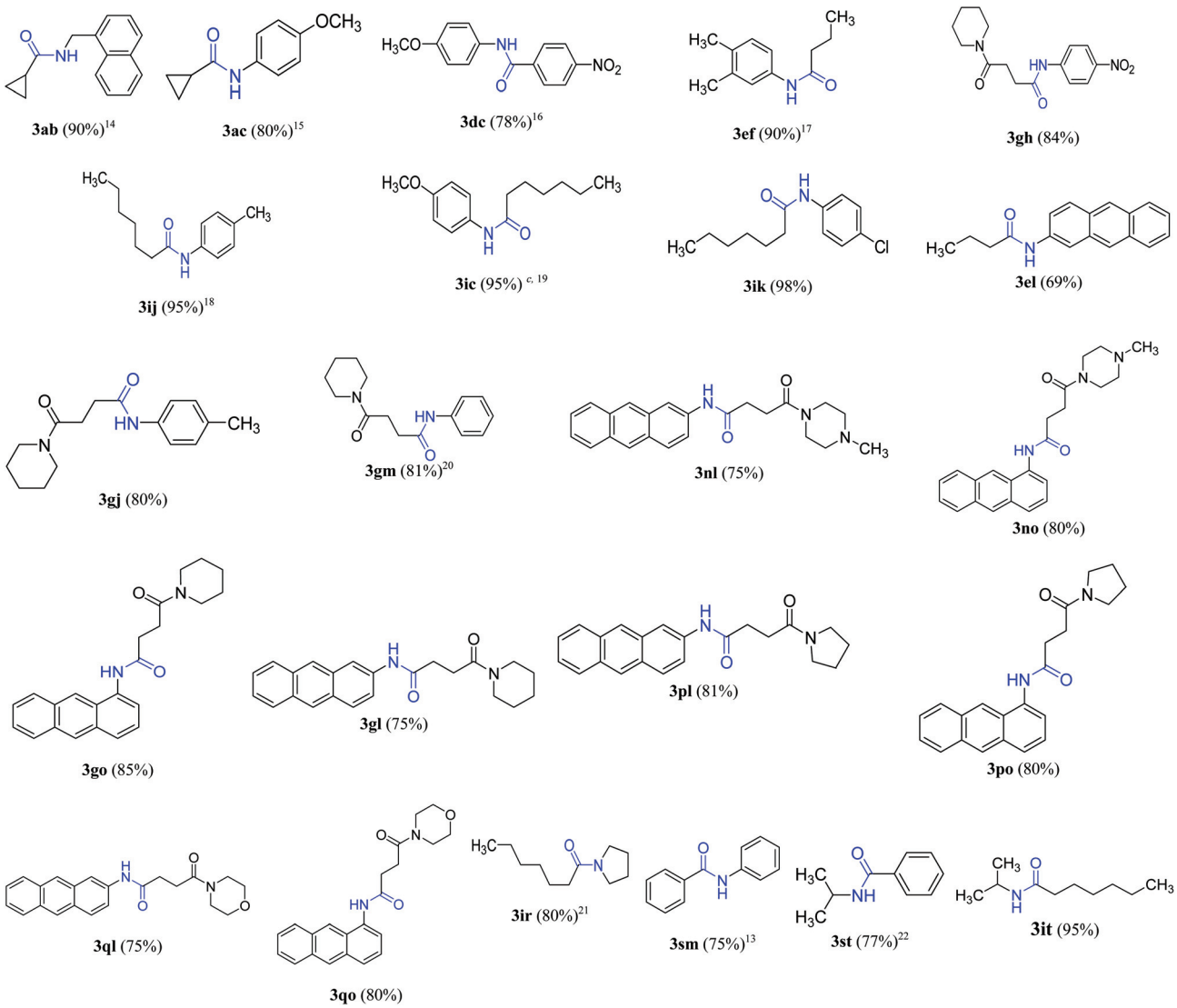

[a] Reaction conditions: **1** (10 mmol), **2** (10 mmol), Alumina balls (10 wt% in relation to total mass of reagents), neat reaction, 140 °C, 3 hours. [b] Isolated yields based on **1**. [c] Reaction was recorded on a 10 mmol scale and also a 100 mmol scale with similar isolated yields.

(255 m^2 g^{-1} surface area and 0.3140 ccg^{-1} pore volume) indicating that it is the ball nature with particular aggregated particle morphology of the alumina that is responsible for the higher catalytic activity. Powder XRD analysis of neutral alumina and the alumina balls activated at different temperatures was also carried out. Powder XRD is due to the particular alumina phase of a sample, which is the same for all samples. So there was only very little difference in the XRD patterns with catalytic activity (Fig. 4). As the activity is dependent on the ball form of the alumina calcined at different temperatures, the powder XRD patterns hardly made any difference. The textural properties of the catalysts as obtained initially from the SEM images and again as measured by N_2 physisorption at 77 K were informative as stated above. These alumina balls are neutral reactants and hence there is no question of protonation of the amines to give an inactive salt. A scale-up reaction was also studied (Table 2, product **3ic**) on a 100 mmol scale with 95% isolated yield. The reaction of *p*-anisidine with heptanoic acid on a 100 mmol scale proceeds just as well as the reaction on a 10 mmol scale. The synthesized aliphatic functionalized acids **p**, **g**, **q** and **n** could survive the present reaction conditions indicating the mildness of the reaction.

Table 3 The summarised porosimetry data as obtained from the N_2 physisorption method[23]

	BET surface area	Pore width	Pore volume
Neutral alumina	88 m^2 g^{-1}	8.18 nm	0.1675 ccg^{-1}
RT alumina ball	255 m^2 g^{-1}	5.68 nm	0.3140 ccg^{-1}
120 °C activated alumina ball	245 m^2 g^{-1}	5.6 nm	0.3136 ccg^{-1}
400 °C activated alumina ball	231 m^2 g^{-1}	6.03 nm	0.3614 ccg^{-1}
700 °C activated alumina ball	122 m^2 g^{-1}	10.8 nm	0.3635 ccg^{-1}

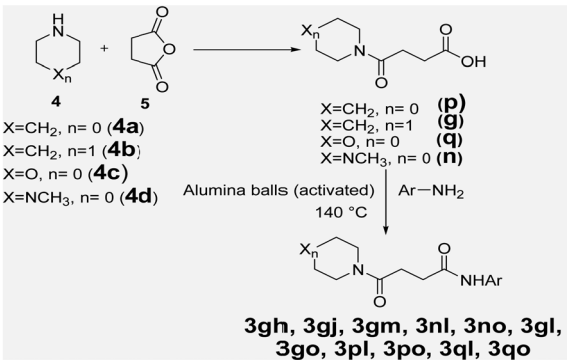

Scheme 1 Synthesis of the carboxylic acids **p**, **g**, **q** and **n** and their corresponding reaction to form the desired amide bond.

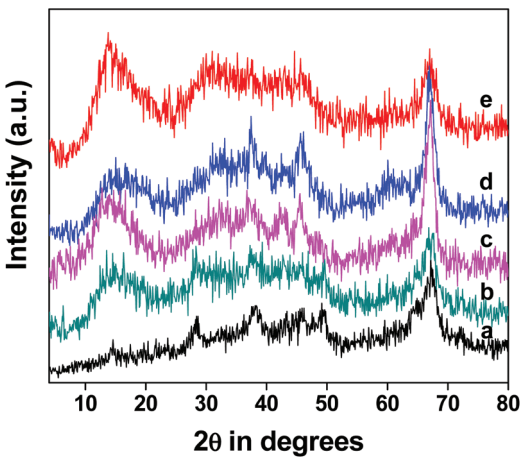

Fig. 4 Wide angle powder XRD patterns of the alumina balls calcined at 120 °C (a); the alumina balls at RT (b); neutral alumina (c); the alumina balls calcined at 700 °C (d) and the alumina balls calcined at 400 °C (e).

The separation and recovery of the catalyst is an important step in the synthesis of fine chemicals, performed generally either by centrifuge or filtration with reduced efficiency. In this catalytic system, because of the macroscopic "ball" nature of the alumina catalyst, it can be recovered simply by filtration. Considering heptanoic acid (4-methoxyphenyl)-amide as the model, the crude reaction mixture is dissolved in dichloromethane and filtered. The alumina balls are further washed and dried under vacuum. These same alumina balls are used for catalysis in a new reaction in order to test its level of reusability (Table 4).

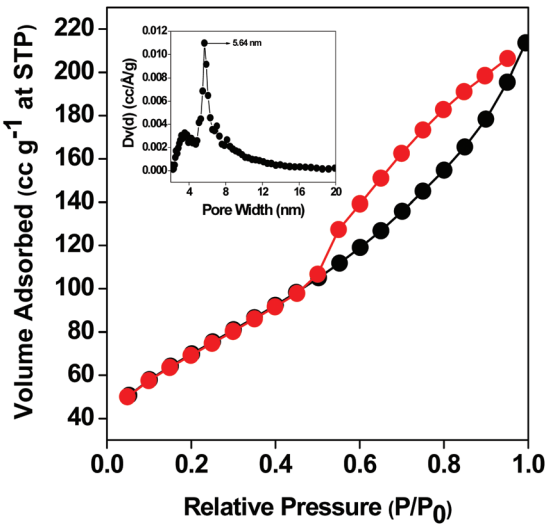

Fig. 5 N_2 adsorption–desorption isotherm of the alumina balls at RT. Pore size distributions estimated through the NLDFT method is shown in the inset. BET surface area of this RT sample is 255 m^2 g^{-1}. Pore width 5.64 nm; pore volume 0.3140 ccg^{-1}.

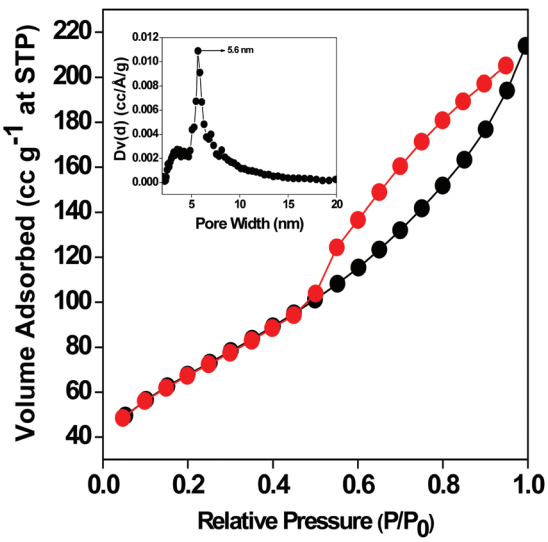

Fig. 6 N_2 adsorption–desorption isotherm of the alumina balls calcined at 120 °C. Pore size distributions estimated through the NLDFT method is shown in the inset. BET surface area of the alumina balls calcined at 120 °C is 245 m^2 g^{-1}. Pore width 5.6 nm; pore volume 0.3136 ccg^{-1}.

Deactivation of the catalyst on storage was also investigated by following the change in activity on long term exposure to the atmosphere (Table 5). The synthesis of heptanoic acid (4-methoxyphenyl)-amide was taken as the model reaction. Even after being exposed for a week the catalyst remains active and gave a yield of 85% without pre-activation to 700 °C. Long term exposure for a month led to 80% yield without pre-treatment.

Table 6 shows a comparison of our alumina ball system with the previously reported K60 silica system for amide syntheses as reported by Clark *et al.*[13] Both are heterogeneous catalysts. Both catalysts deliver the best results when activated at 700 °C.

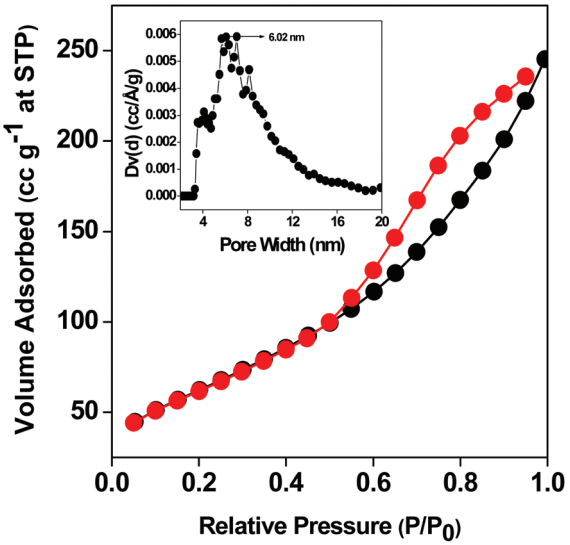

Fig. 7 N_2 adsorption–desorption isotherm of the alumina balls calcined at 400 °C. Pore size distributions estimated through the NLDFT method is shown in the inset. BET surface area of the alumina balls calcined at 400 °C is 231 m^2 g^{-1}. Pore width 6.03 nm; pore volume 0.3614 ccg^{-1}.

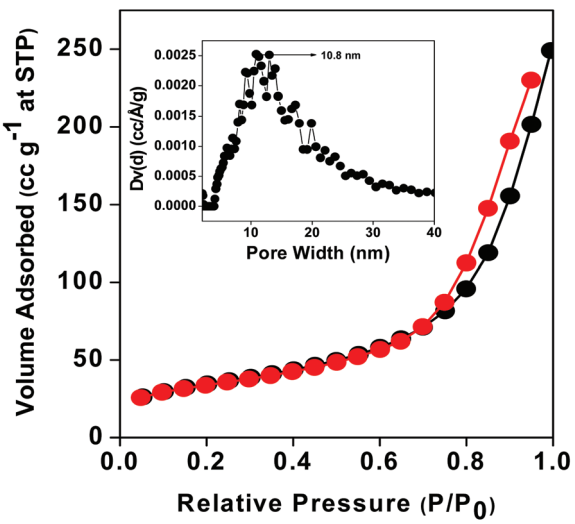

Fig. 8 N_2 adsorption–desorption isotherm of the alumina balls calcined at 700 °C. Pore size distributions estimated through the NLDFT method is shown in the inset. BET surface area of the alumina balls calcined at 700 °C is 122 m^2 g^{-1}. Pore width 10.8 nm; pore volume 0.3635 ccg^{-1}.

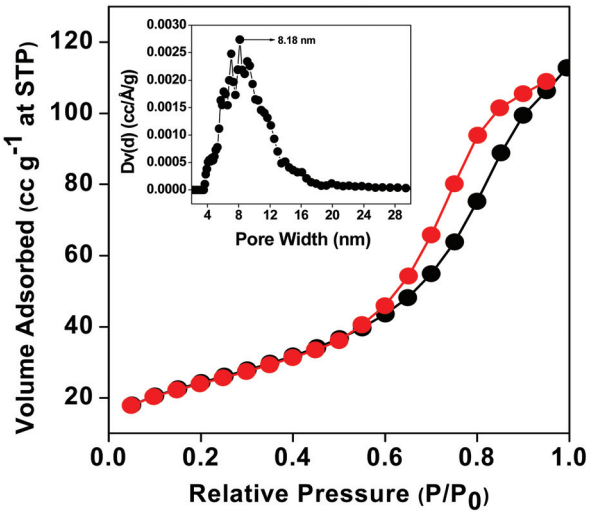

Fig. 9 N_2 adsorption–desorption isotherm of neutral alumina. Pore size distributions estimated through the NLDFT method is shown in the inset. BET surface area of neutral alumina is 88 m^2 g^{-1}. Pore width 8.18 nm; pore volume 0.1675 ccg^{-1}.

Table 4 Effect of reuse on yield of heptanoic acid (4-methoxy-phenyl)-amide[a,b]

Reactivation temperature	1st use Yield[c] (%)	2nd use	3rd use
CH_2Cl_2 wash (dried under vacuum)	85	82	81
120 °C	88	85	83
700 °C	90	90	88

[a] Reaction conditions as in Table 3. [b] There was no loss of catalyst on transfer due to the macroscopic "ball" nature of the catalyst. [c] Recrystallized isolated yield.

Table 5 Change in isolated yield of heptanoic acid (4-methoxyphenyl)-amide with time[a,b]

	Time of exposure in air			
	12 hours	24 hours	1 week	1 month
Unactivated catalyst	90	88	85	80
Activated catalyst (700 °C)	93	93	89	85

[a] Reaction conditions as in Table 3. [b] Recrystallized isolated yield given under each column.

However, our alumina ball catalyst also gives comparable yields when activated at 400 °C. Thus, our catalyst can function at a considerably lower calcination temperature. K60 silica requires refluxing toluene for promoting the amide bond formation. Alumina balls as catalyst can promote the same reaction using a solvent free methodology (see Table 6). On average, a 20 wt% catalyst loading is required for optimal yields in the case of K60 silica.[13] The catalyst loading for the alumina balls is only 10 wt%. Many factors must be considered when designing cleaner synthetic routes. Table 6 also gives a comparison based on established green chemistry metrics.[24] This shows that alumina balls activated at 700 °C are substantially cleaner and more efficient than the alternative heterogeneous K60 methodology, especially in terms of the ratio of waste to product (E-factor in our alumina balls catalysed reaction is 0.15 for compound **3sm**, see Table 6) and mass intensity (MI 1.60 for compound **3sm** in our methodology, Table 6). In an ideal situation, the mass intensity would approach 1. Therefore, the green metrics of this present methodology is much more towards the ideal results. The challenge for green chemistry and green engineering is to

Table 6 A comparison of efficiency between catalysts in the synthesis of *N*-phenyl-benzamide (**3sm**)[a]

Catalyst	Catalyst loading (wt%)	Solvent	Yield[b] (%)	E-factor	Mass intensity	Atom economy (%)
K60 silica[12]	50	Toluene	47	2.73	19.13	92
Alumina ball[c]	10	—	75	0.15	1.60	92

[a] 10 mmol each of the starting materials benzoic acid and aniline, neat reaction, 140 °C, 3 hours for the reaction with alumina ball catalyst. [b] Isolated yield. [c] Calcined at 700 °C.

decrease significantly the material intensities observed, for example, the mass intensity by at least an order of magnitude, if not more. It is better to prevent waste than to treat or cleanup waste after it is formed.

Conclusions

In conclusion, the present methodology opens up an interesting and attractive sustainable avenue for the synthesis of amide functionalities. We use a solvent-free protocol for amide bond formation using non-toxic, inexpensive and biocompatible alumina balls. The advantage of this environmentally benign and safe protocol includes a simple reaction setup which does not require any specialised equipment, mild reaction conditions, high product yields, short reaction times, the possibility for reusing the catalyst and solvent-free conditions. As we learn better ways to synthesize complex, highly functionalized amide-based structures without the need for aggressive reactants and cumbersome protecting groups, synthetic amides will provide a new generation of functional materials with controllable higher-order properties.

Experimental section

General information

Amides were synthesized under neat reaction conditions at 140 °C and an air atmosphere. The typical quantities used were 10 mmols of acid, 10 mmols of amine, and varying quantities of activated alumina ball catalyst. NMR spectra were obtained on a 300 MHz Bruker spectrometer using $CDCl_3$ or DMSO-d_6 solvent. Powder X-ray diffraction patterns of the samples were analyzed by using a Philips X'Pert PRO Diffractometer. Nitrogen adsorption–desorption isotherms of the samples were recorded on a Quantachrome Autosorb 1C, at 77 K. Prior to the gas adsorption measurements, the samples were degassed at 473 K for 6 hours under high vacuum.

General procedure for amide synthesis

Cyclopropanecarboxylic acid (naphthalen-1-ylmethyl)-amide (3ab). Cyclopropanecarboxylic acid (0.80 ml, 10 mmol), *C*-naphthalen-1-yl-methylamine (1.47 ml, 10 mmol) and activated alumina balls calcined at 700 °C (243.3 mg) were heated to 140 °C in a round bottomed flask. After 3 hours the hot reaction mixture was diluted with ethyl acetate and filtered through a sintered glass funnel, the catalyst was washed with 20 ml of hot ethyl acetate and dried under vacuum. The yield obtained for cyclopropanecarboxylic acid (naphthalen-1-ylmethyl)-amide was 2.03 g (90%).

Amide analytical data

Cyclopropanecarboxylic acid (naphthalen-1-ylmethyl)-amide (3ab). White solid; m.p. 167 °C (EtOAc); ^{1}H NMR (300 MHz, DMSO-d_6): δ 8.54 (br s, 1H, N*H*), 8.02 (d, J = 7.2 Hz, 1H, Ar), 7.91 (d, J = 8.1 Hz, 1H, Ar), 7.82 (d, J = 7.2 Hz, 1H, Ar), 7.52–7.42 (m, 4H), 4.71 (d, J = 5.4 Hz, 2H, benzylic), 1.59–1.58 (m, 1H), 0.69–0.61 (m, 4H); ^{13}C NMR (75 MHz, DMSO-d_6): δ 172.5, 134.9, 133.4, 131.0, 128.5, 127.6, 126.3, 125.8, 125.7, 125.5, 123.6, 13.6, 6.3; IR(KBr) 3296 (NH), 1627 (C═O), 1537 (NH *def*) cm^{-1}; Anal. calcd for $C_{15}H_{15}NO$: C, 79.97; H, 6.71; N, 6.22 and found C, 79.99; H, 6.70; N, 6.25.

Cyclopropanecarboxylic acid (4-methoxy-phenyl)-amide (3ac). Blue solid; m.p. 127 °C (EtOAc); ^{1}H NMR (300 MHz, $CDCl_3$): δ 7.92 (br s, 1H, N*H*), 7.38 (d, J = 8.7 Hz, 2H, Ar), 6.79 (d, J = 8.4 Hz, 2H, Ar), 3.75 (s, 3H, OC*H*$_3$), 1.50–1.48 (m, 1H), 1.01 (m, 2H), (m, 2H); ^{13}C NMR (75 MHz, $CDCl_3$): δ 172.1, 156.1, 131.4, 121.8, 114.0, 55.4, 15.3, 7.6; IR(KBr) 3299 (NH), 1652 (C═O), 1524 (NH *def*) cm^{-1}; Anal. calcd for $C_{11}H_{13}NO_2$: C, 69.09; H, 6.85; N, 7.32 and found C, 69.10; H, 6.86; N, 7.34.

***N*-(4-Methoxyphenyl)-4-nitrobenzamide (3dc).** Yellow solid; m.p. 199 °C (MeOH); ^{1}H NMR (300 MHz, DMSO-d_6) δ 8.32 (d, J = 8.7 Hz, 2H, Ar), 8.04 (d, J = 8.7 Hz, 2H, Ar), 7.88 (s, 1H, N*H*), 7.55 (d, J = 8.9 Hz, 2H, Ar), 6.93 (d, J = 8.9 Hz, 2H, Ar), 3.75 (s, OC*H*$_3$, 3H,); ^{13}C NMR (75 MHz, DMSO-d_6) δ 163.3, 155.9, 149.0, 140.7, 131.7, 129.0, 123.4, 122.1, 113.8, 55.1; IR(KBr) 2932 (NH), 1621 (C═O) cm^{-1}; Anal. calcd for $C_{14}H_{12}N_2O_4$: C, 61.76; H, 4.44; N, 10.29 and found C, 61.73; H, 4.47; N, 10.30.

***N*-(3,4-Dimethylphenyl)-butyramide (3ef).** Brown solid; m.p. 60 °C (EtOAc); ^{1}H NMR (300 MHz, $CDCl_3$): δ 7.95 (br s, 1H, N*H*), 7.32 (s, 1H, Ar), 7.25 (d, J = 9 Hz, 1H, Ar), 7.02 (d, J = 7.8 Hz, 1H, Ar), 2.32 (t, J = 7.2 Hz, 2H), 2.19 (s, 3H, Ar C*H*$_3$), 1.77–1.74 (m, 2H) and 0.97 (t, J = 7.5 Hz, 3H); ^{13}C NMR (75 MHz, $CDCl_3$): δ 171.8, 136.9, 135.6, 132.4, 129.7, 121.6, 117.7, 39.2, 19.7, 19.1, 19.0 and 13.6; IR(KBr) 3300 (NH), 1660 (C═O) cm^{-1}; Anal. calcd for $C_{12}H_{17}NO$: C, 75.35; H, 8.96; N, 7.32 and found C, 75.33; H, 8.93; N, 7.35.

***N*-(4-Nitrophenyl)-4-oxo-4-piperidin-1-yl-butyramide (3gh).** White solid; m.p. 180 °C ($CHCl_3$); ^{1}H NMR (300 MHz, $CDCl_3$): δ 10.05 (br s, 1H, N*H*), 8.10 (d, J = 9 Hz, 2H, Ar), 7.69 (d, J = 9 Hz, 2H, Ar), 3.59–3.49 (m, 4H), 2.83 (s, 4H), 1.66–1.61 (m, 6H). ^{13}C NMR (75 MHz, $CDCl_3$): δ 171.1, 170.4,

138.6, 128.7, 124.8, 119.1, 46.5, 43.1, 32.7, 28.9, 26.3, 25.5, 24.2; IR(KBr) 2931 (NH), 1623 (C═O) cm^{-1}; Anal. calcd for $C_{15}H_{19}N_3O_4$: C, 59.01; H, 6.27; N, 13.76 and found C, 59.04; H, 6.27; N, 13.75.

Heptanoic acid *p*-tolylamide (3ij). Light brown solid; m.p. 80 °C (EtOAc); ^{1}H NMR (300 MHz, $CDCl_3$): δ 7.76 (br s, 1H, N*H*), 7.39 (d, J = 7.5 Hz, 2H, Ar), 7.08 (d, J = 7.5 Hz, 2H, Ar), 2.35–2.29 (m, 5H, Ar CH_3 and COCH_2), 1.69 (m, 2H), 1.29 (br s, 6H), 0.85 (t, J = 6.6 Hz, 3H); ^{13}C NMR (75 MHz, $CDCl_3$): δ 171.7, 135.4, 133.6, 129.3, 120.1, 37.6, 31.5, 28.9, 25.6, 22.4, 20.7, 13.9; IR(KBr) 3314 (NH), 1659 (C═O) cm^{-1}; Anal. calcd for $C_{14}H_{21}NO$: C, 76.67; H, 9.65; N, 6.39 and found C, 76.67; H, 9.65; N, 6.40.

Heptanoic acid (4-methoxyphenyl)-amide (3ic). Light brown solid; m.p. 70 °C (EtOAc); ^{1}H NMR (300 MHz, $CDCl_3$): δ 8.04 (br s, 1H, N*H*), 7.40 (d, J = 8.7 Hz, 2H, Ar), 6.79 (d, J = 8.7 Hz, 2H, Ar), 3.75 (s, 3H), 2.31 (t, J = 7.5 Hz, 2H), 1.69–1.62 (m, 2H), 1.27 (br s, 6H), 0.85 (t, J = 6.6 Hz, 3H); ^{13}C NMR (75 MHz, $CDCl_3$): δ 172.0, 156.4, 130.9, 122.1, 114.0, 55.4, 37.3, 31.5, 28.9, 25.8, 22.4, 13.9; IR(KBr) 3316 (NH), 1654 (C═O) cm^{-1}; Anal. calcd for $C_{14}H_{21}NO_2$: C, 71.46; H, 8.99; N, 5.95 and found C, 71.47; H, 9.00; N, 5.95.

Heptanoic acid (4-chlorophenyl)-amide (3ik). Light brown solid; m.p. 174 °C (EtOAc); ^{1}H NMR (300 MHz, $CDCl_3$): δ 7.45 (br s, 1H, N*H*), 7.39 (d, J = 8.7 Hz, 2H, Ar), 7.18 (d, J = 8.4 Hz, 2H, Ar), 2.26 (t, J = 7.5 Hz, 2H), 1.67–1.53 (m, 2H), 1.22 (br s, 6H), 0.81 (t, J = 6.9 Hz, 3H); ^{13}C NMR (75 MHz, $CDCl_3$): δ 171.7, 136.5, 129.2, 128.9, 121.1, 37.7, 31.5, 28.9, 25.5, 22.5, 14.0; IR(KBr) 3310 (NH), 1659 (C═O) cm^{-1}; Anal. calcd for $C_{13}H_{18}ClNO$: C, 65.13; H, 7.57; N, 5.84 and found C, 65.15; H, 7.57; N, 5.83.

***N*-Anthracen-2-yl-butyramide (3el).** Yellow solid; m.p. above 260 °C (MeOH); ^{1}H NMR (300 MHz, DMSO-d_6): δ 10.09 (s, 1H, N*H*), 8.48–8.35 (m, 3H, Ar), 8.00–7.93 (m, 3H, Ar), 7.52 (d, J = 9.6 Hz, 1H, Ar), 7.43 (m, 2H, Ar), 2.34 (t, J = 7.8 Hz, 2H), 1.67–1.60 (m, 2H), 0.92 (t, J = 7.5 Hz, 3H); ^{13}C NMR (75 MHz, DMSO-d_6): δ 171.3, 136.5, 131.8, 130.4, 128.8, 128.5, 128.2, 127.8, 125.9, 125.7, 124.9, 121.1, 113.5, 39.2, 19.7, 19.2, and 13.7; IR(KBr) 3410 (NH), 1627 (C═O) cm^{-1}; Anal. calcd for $C_{18}H_{17}NO$: C, 82.10; H, 6.51; N, 5.32 and found C, 82.12; H, 6.52; N, 5.30.

4-Oxo-4-piperidin-1-yl-*N*-*p*-tolyl-butyramide (3gj). White solid; m.p. 134 °C ($CHCl_3$); ^{1}H NMR (300 MHz, $CDCl_3$): δ 9.02 (s, 1H, N*H*), 7.36 (d, J = 8.4 Hz, 2H, Ar), 6.98 (d, J = 8.4 Hz, 2H, Ar), 3.48 (br s, 2H), 3.35 (br s, 2H), 2.68 (s, 4H), 2.21 (s, 3H, Ar CH_3), 1.56–1.47 (m, 6H); ^{13}C NMR (75 MHz, $CDCl_3$): δ 170.9, 170.5, 136.0, 133.2, 130.1, 129.2, 123.2, 119.8, 46.6, 43.1, 32.7, 28.9, 26.3, 25.5, 24.4, 20.8; IR(KBr) 3270 (NH), 1623 (C═O) cm^{-1}; Anal. calcd for $C_{16}H_{22}N_2O_2$: C, 70.04; H, 8.08; N, 10.21 and found C, 70.05; H, 8.09; N, 10.21.

4-Oxo-*N*-phenyl-4-piperidin-1-yl-butyramide (3gm). White solid; m.p. 123 °C ($CHCl_3$); ^{1}H NMR (300 MHz, $CDCl_3$): δ 9.08 (s, 1H, N*H*), 7.48 (d, J = 8.1 Hz, 2H, Ar), 7.21–7.15 (m, 2H, Ar), 6.98–6.93 (m, 1H, Ar), 3.48 (br s, 2H), 3.35 (br s, 2H), 2.68 (s, 4H), 1.56–1.44 (m, 6H); ^{13}C NMR (75 MHz, $CDCl_3$): δ 171.1, 170.4, 138.6, 128.7, 123.6, 123.3, 119.7, 46.5, 43.1, 32.7, 28.9, 26.3, 25.5, 24.4; IR(KBr) 3270 (NH), 1622 (C═O) cm^{-1}; Anal. calcd for $C_{15}H_{20}N_2O_2$: C, 69.20; H, 7.74; N, 10.76 and found C, 69.21; H, 7.74; N, 10.77.

***N*-Anthracen-2-yl-4-(4-methyl-piperazin-1-yl)-4-oxo-butyramide (3nl).** Greenish-brown solid; m.p. 141 °C (DMSO); ^{1}H NMR (300 MHz, DMSO-d_6): δ 10.21 (s, 1H, N*H*), 8.45 (d, J = 9.3 Hz, 2H, Ar), 8.36 (s, 1H, Ar), 7.99 (d, J = 9.0 Hz, 3H, Ar), 7.53 (dd, J = 9.0, 1.8 Hz, 1H, Ar), 7.46–7.38 (m, 2H, Ar), 3.44–3.40 (m, 4H), 2.62 (br s, 4H), 2.28 (br s, 2H), 2.21–2.18 (m, 2H), 2.14 (s, 3H); ^{13}C NMR (75 MHz, DMSO-d_6): δ 171.2, 169.8, 136.5, 131.8, 130.4, 128.7, 128.5, 128.1, 127.7, 125.9, 125.6, 124.9, 121.1, 113.5, 54.8, 54.4, 45.7, 44.7, 41.1, 31.6, 27.7; IR(KBr) 3263 (NH), 1650 (C═O) cm^{-1}; Anal. calcd for $C_{23}H_{25}N_3O_2$: C, 73.57; H, 6.71; N, 11.19 and found C, 73.55; H, 6.70; N, 11.21.

***N*-Anthracen-1-yl-4-(4-methyl-piperazin-1-yl)-4-oxo-butyramide (3no).** Reddish-brown sticky solid; ^{1}H NMR (300 MHz, DMSO-d_6): δ 10.06 (s, 1H, N*H*), 8.79 (s, 1H, Ar), 8.54 (s, 1H, Ar), 8.05 (br s, 2H, Ar), 7.88–7.87 (m, 1H, Ar), 7.68 (br s, 1H, Ar), 7.49 (br s, 3H, Ar), 3.45 (br s, 4H), 2.75–2.70 (m, 4H), 2.26–2.21 (m, 4H), 2.13 (s, 3H); ^{13}C NMR (75 MHz, DMSO-d_6): δ 171.5, 170.0, 133.9, 131.9, 131.1, 131.0, 128.4, 127.9, 126.4, 125.9, 125.8, 125.2, 121.7, 120.0, 117.8, 54.8, 54.4, 45.7, 44.7, 41.2, 31.3, 27.9; IR(KBr) 3259 (NH), 1641 (C═O) cm^{-1}; Anal. calcd for $C_{23}H_{25}N_3O_2$: C, 73.57; H, 6.71; N, 11.19 and found C, 73.58; H, 6.69; N, 11.19.

***N*-Anthracen-2-yl-4-oxo-4-piperidin-1-yl-butyramide (3gl).** Greenish-brown solid; m.p. 165 °C (DMSO); ^{1}H NMR (300 MHz, DMSO-d_6): δ 10.02 (s, 1H, N*H*), 8.29 (d, J = 9.3 Hz, 2H, Ar), 8.21 (s, 1H, Ar), 7.83 (d, J = 9.0 Hz, 3H, Ar), 7.37 (d, J = 9.0 Hz, 1H, Ar), 7.31–7.25 (m, 2H, Ar), 3.25–3.21 (m, 4H), 2.31 (br s, 4H), 1.40–1.36 (m, 4H), 1.22 (br s, 2H); ^{13}C NMR (75 MHz, DMSO-d_6): δ 171.3, 169.4, 136.5, 131.8, 130.4, 128.8, 128.5, 128.2, 127.8, 125.9, 125.7, 124.9, 121.1, 113.5, 45.8, 42.1, 31.7, 27.6, 26.1, 25.4, 24.2; IR(KBr) 3267 (NH), 1646 (C═O) cm^{-1}; Anal. calcd for $C_{23}H_{24}N_2O_2$: C, 76.64; H, 6.71; N, 7.77 and found C, 76.65; H, 6.74; N, 7.75.

***N*-Anthracen-1-yl-4-oxo-4-piperidin-1-yl-butyramide (3go).** Yellow solid; m.p. 161 °C (DMSO); ^{1}H NMR (300 MHz, DMSO-d_6): δ 10.02 (s, 1H, N*H*), 8.79 (s, 1H, Ar), 8.55 (s, 1H, Ar), 8.06–8.03 (m, 2H, Ar), 7.87 (d, J = 8.7 Hz, 1H, Ar), 7.68 (d, J = 6.6 Hz, 1H, Ar), 7.51–7.44 (m, 3H, Ar), 3.43–3.42 (m, 4H), 2.76–2.68 (m, 4H), 1.54–1.40 (m, 6H); ^{13}C NMR (75 MHz, DMSO-d_6): δ 171.7, 169.7, 133.9, 132.0, 131.2, 131.0, 128.4, 127.9, 126.6, 126.4, 125.9, 125.3, 121.8, 120.1, 45.9, 42.2, 31.4, 28.0, 26.1, 25.5, 24.2; IR(KBr) 3275 (NH), 1640 (C═O), 1533 (NH *def*) cm^{-1}; Anal. calcd for $C_{23}H_{24}N_2O_2$: C, 76.64; H, 6.71; N, 7.77 and found C, 76.61; H, 6.74; N, 7.77.

***N*-Anthracen-2-yl-4-oxo-4-pyrrolidin-1-yl-butyramide (3pl).** Brown solid; m.p. 200 °C (MeOH); ^{1}H NMR (300 MHz, $CDCl_3$): δ 9.86 (s, 1H, N*H*), 8.49 (s, 1H, Ar), 8.26 (s, 2H, Ar), 7.90–7.85 (m, 3H, Ar), 7.52–7.40 (m, 3H, Ar), 3.47 (t, J = 6.0 Hz, 4H), 2.82–2.71 (m, 4H), 2.03–1.85 (m, 4H); ^{13}C NMR (75 MHz, $CDCl_3$): δ 170.9, 169.8, 135.3, 131.5, 131.3, 130.1,

128.3, 128.0, 127.5, 127.1, 125.2, 124.8, 124.6, 124.1, 120.6, 114.1, 45.9, 45.2, 31.5, 29.3, 25.3, 23.7; IR(KBr) 3293 (NH), 1621 (C═O) cm^{-1}; Anal. calcd for $C_{22}H_{22}N_2O_2$: C, 76.28; H, 6.40; N, 8.09 and found C, 76.28; H, 6.42; N, 8.09.

***N*-Anthracen-1-yl-4-oxo-4-pyrrolidin-1-yl-butyramide (3po).** Brown solid; m.p. 190 °C (MeOH); ^{1}H NMR (300 MHz, $CDCl_3$): δ 9.66 (s, 1H, N*H*), 8.74 (s, 1H, Ar), 8.42 (s, 1H, Ar), 8.15–7.98 (m, 3H, Ar), 7.80 (d, J = 8.4 Hz, 1H, Ar), 7.49–7.42 (m, 3H, Ar), 3.62 (t, J = 6.9 Hz, 2H), 3.46 (t, J = 6.6 Hz, 2H), 2.98–2.95 (m, 2H), 2.88–2.82 (m, 2H), 2.01–1.79 (m, 4H); ^{13}C NMR (75 MHz, DMSO-d_6): δ 171.7, 169.9, 133.9, 132.0, 131.2, 131.0, 128.4, 127.9, 126.4, 125.9, 125.3, 121.7, 120.0, 46.0, 45.5, 31.1, 29.4, 25.7, 24.1; IR(KBr) 3265 (NH), 1627 (C═O), 1542 (NH *def*) cm^{-1}; Anal. calcd for $C_{22}H_{22}N_2O_2$: C, 76.28; H, 6.40; N, 8.09 and found C, 76.30; H, 6.42; N, 8.09.

***N*-Anthracen-2-yl-4-morpholin-4-yl-4-oxo-butyramide (3ql).** Brown solid, m.p. 190 °C (DMSO); ^{1}H NMR (300 MHz, DMSO-d_6): δ 10.19 (s, 1H, N*H*), 8.48–8.37 (m, 3H, Ar), 8.00–7.97 (m, 3H, Ar), 7.53 (d, J = 8.1 Hz, 1H, Ar), 7.42 (br s, 2H, Ar), 3.55–3.41 (m, 8H), 2.64 (s, 4H); ^{13}C NMR (75 MHz, DMSO-d_6): δ 171.1, 170.1, 142.2, 136.4, 131.8, 130.4, 128.8, 128.5, 128.1, 127.7, 125.8, 125.6, 124.9, 121.1, 113.5, 66.2, 45.3, 41.6, 31.5, 27.5; IR(KBr) 3252 (NH), 1653 (C═O) cm^{-1}; Anal. calcd for $C_{22}H_{22}N_2O_3$: C, 72.91; H, 6.12; N, 7.73 and found C, 72.90; H, 6.12; N, 7.70.

***N*-Anthracen-1-yl-4-morpholin-4-yl-4-oxo-butyramide (3qo).** Brown solid, m.p. 185 °C (MeOH); ^{1}H NMR (300 MHz, $CDCl_3$): δ 9.17 (s, 1H, N*H*), 8.61 (s, 1H, Ar), 8.42 (s, 1H, Ar), 8.07–8.01 (m, 3H, Ar), 7.89 (d, J = 8.4 Hz, 1H, Ar), 7.49–7.41 (m, 3H, Ar), 3.96–3.87 (m, 6H), 3.70–3.65 (m, 2H), 2.98–2.96 (m, 2H), 2.85–2.84 (m, 2H); ^{13}C NMR (75 MHz, $CDCl_3$): δ 171.5, 170.9, 132.7, 132.1, 131.5, 131.4, 128.4, 127.8, 126.8, 125.9, 125.6, 125.3, 125.0, 120.0, 118.8, 66.6, 66.3, 45.6, 42.1, 32.5, 29.0; IR(KBr) 3276 (NH), 1654 (C═O) cm^{-1}; Anal. calcd for $C_{22}H_{22}N_2O_3$: C, 72.91; H, 6.12; N, 7.73 and found C, 72.90; H, 6.12; N, 7.75.

1-Pyrrolidin-1-yl-heptan-1-one (3ir). Brown liquid, b.p. 297 ± 5 °C (760 mm Hg pressure); ^{1}H NMR (300 MHz, $CDCl_3$): δ 3.42–3.34 (m, 4H, NCH_2), 2.20 (t, J = 7.5 Hz, 2H), 1.93–1.74 (m, 4H, NCH$_2$CH_2), 1.60–1.53 (m, 2H), 1.32–1.24 (m, 6H), 0.83 (t, J = 6.9 Hz, 3H); ^{13}C NMR (75 MHz, $CDCl_3$): δ 176.4, 46.6, 45.6, 34.8, 31.6, 29.1, 26.1, 24.9, 24.4, 22.5, 14.0; IR (KBr) 3442 (NH), 1613 (C═O) cm^{-1}; Anal. calcd for $C_{11}H_{21}NO$: C, 72.08; H, 11.55; N, 7.64 and found C, 72.08; H, 11.52; N, 7.63.

***N*-Phenyl-benzamide (3sm).** White solid, m.p. 165 °C (CH_2Cl_2); ^{1}H NMR (300 MHz, $CDCl_3$): δ 8.02 (s, 1H, N*H*), 7.86 (d, J = 7.5 Hz, 2H, Ar), 7.65 (d, J = 7.8 Hz, 2H, Ar), 7.53 (t, J = 7.2 Hz, 1H, Ar), 7.45 (t, J = 7.8 Hz, 2H, Ar), 7.36 (t, J = 7.8 Hz, 2H, Ar), 7.15 (t, J = 7.5 Hz, 1H, Ar); ^{13}C NMR (75 MHz, $CDCl_3$): δ 165.9, 137.9, 134.9, 131.8, 129.0, 128.6, 127.0, 124.5, 120.3; IR(KBr) 3342 (NH), 1653 (C═O) cm^{-1}; Anal. calcd for $C_{13}H_{11}NO$: C, 79.16; H, 5.62; N, 7.10 and found C, 79.18; H, 5.62; N, 7.12.

***N*-Isopropylbenzamide (3st).** White solid, m.p. 102 °C (EtOAc); ^{1}H NMR (300 MHz, $CDCl_3$): δ 7.75 (d, J = 7.2 Hz, 2H, Ar), 7.47–7.35 (m, 3H, Ar), 6.22 (br s, 1H, N*H*), 4.30–4.24 (m, 1H), 1.24 (d, J = 6.3 Hz, 6H); ^{13}C NMR (75 MHz, $CDCl_3$): δ 166.8, 134.8, 131.1, 128.4, 126.8, 41.8, 22.7; IR(KBr) 3299 (NH), 1631 (C═O), 1534 (NH *def*) cm^{-1}; Anal. calcd for $C_{10}H_{13}NO$: C, 73.59; H, 8.03; N, 8.58 and found C, 73.56; H, 8.01; N, 8.60.

***N*-Isopropylheptanamide (3it).** Brown sticky liquid, ^{1}H NMR (300 MHz, $CDCl_3$): δ 5.88 (br s, 1H, N*H*), 4.04–3.93 (m, 1H), 2.06 (t, J = 7.5 Hz, 2H), 1.55–1.48 (m, 2H), 1.20 (s, 6H), 1.06 (d, J = 6.3 Hz, 6H), 0.81 (t, J = 6.0 Hz, 3H); ^{13}C NMR (75 MHz, $CDCl_3$): δ 172.3, 41.0, 36.7, 31.4, 28.7, 25.7, 22.5, 22.3, 13.8; IR(KBr) 3287 (NH), 1643 (C═O), 1550 (NH *def*) cm^{-1}; Anal. calcd for $C_{10}H_{21}NO$: C, 70.12; H, 12.36; N, 8.18 and found C, 70.13; H, 12.36; N, 8.20.

Acknowledgements

One of the authors (SG) thanks the UGC, New Delhi, for her fellowship (SRF). We also acknowledge the grant received from the UGC funded Major project, F. no. 37-398/2009 (SR) dated 11-01-2010.

Notes and references

1 (*a*) E. Valeur and M. Bradley, *Chem. Soc. Rev.*, 2009, **38**, 606; (*b*) A. Greenberg, C. M. Breneman and J. F. Liebman, *The Amide Linkage: Structural Significance in Chemistry, Biochemistry, and Materials Science*, John Wiley & Sons, New York, 1999; (*c*) J. Rebek, *Acc. Chem. Res.*, 1999, **32**, 278; (*d*) R. P. Cheng, S. H. Gellman and W. F. DeGrado, *Chem. Rev.*, 2001, **101**, 3219; (*e*) D. J. Hill, M. J. Mio, R. B. Prince, T. S. Hughes and J. S. Moore, *Chem. Rev.*, 2001, **101**, 3893.
2 (*a*) C. A. G. N. Montalbetti and V. Falque, *Tetrahedron*, 2005, **61**, 10827; (*b*) A. K. Ghose, V. N. Viswanadhan and J. J. Wendoloski, *J. Comb. Chem.*, 1999, **1**, 55.
3 (*a*) D. J. C. Constable, P. J. Dunn, J. D. Hayler, G. R. Humphrey, J. Leazer, R. J. Linderman, K. Lorenz, J. Manley, B. A. Pearlman, A. Wells, A. Zaks and T. Y. Zhang, *Green Chem.*, 2007, **9**, 411; (*b*) J. S. Carey, D. Laffan, C. Thomson and M. T. Williams, *Org. Biomol. Chem.*, 2006, **4**, 2337.
4 (*a*) S. Y. Han and Y. A. Kim, *Tetrahedron*, 2004, **60**, 2447.
5 W. K. Chan, C. M. Ho, M. K. Wong and C. M. Che, *J. Am. Chem. Soc.*, 2006, **128**, 14796.
6 (*a*) W. J. Yoo and C. J. Li, *J. Am. Chem. Soc.*, 2006, **128**, 13064; (*b*) K. Ekour-Kovi and C. Wolf, *Org. Lett.*, 2007, **9**, 3429; (*c*) J. Gao and G. W. Wang, *J. Org. Chem.*, 2008, **73**, 2955; (*d*) A. Tillack, I. Rudloff and M. Beller, *Eur. J. Org. Chem.*, 2001, 523.
7 (*a*) C. Gunanathan, Y. Ben-David and D. Milstein, *Science*, 2007, **317**, 790; (*b*) L. U. Nordstrøm, H. Vogt and R. Madsen, *J. Am. Chem. Soc.*, 2008, **130**, 17672; (*c*) A. J. A. Watson, A. C. Maxwell and J. M. J. Williams, *Org. Lett.*, 2009, **11**, 2667; (*d*) T. Zweifel, J. V. Naubron and H. Grützmacher, *Angew. Chem., Int. Ed.*, 2009, **48**, 559.
8 (*a*) P. Daw, A. Sinha, S. M. W. Rahaman, S. Dinda and J. K. Bera, *Organometallics*, 2012, **31**, 3790; (*b*) T. Tu, Z. Wang, Z. Liu, X. Feng and Q. Wang, *Green Chem.*, 2012, **14**, 921.
9 J. Cossy and C. Palegrosdemange, *Tetrahedron Lett.*, 1989, **30**, 2771.
10 L. J. Gooßen, D. M. Ohlmann and P. P. Lange, *Synthesis*, 2009, 160.
11 K. Arnold, B. Davies, R. L. Giles, C. Grosjean, G. E. Smith and A. Whiting, *Adv. Synth. Catal.*, 2006, **348**, 813.
12 H. Charville, D. A. Jackson, G. Hodges, A. Whiting and M. R. Wilson, *Eur. J. Org. Chem.*, 2011, 5981.
13 J. W. Comerford, J. H. Clark, D. J. Macquarrie and S. W. Breeden, *Chem. Commun.*, 2009, 2562.
14 G. A. Molander and F. Beaumard, *Org. Lett.*, 2011, **13**(5), 1242.

15 J. S. Yadav, B. V. Subba Reddy, U. V. Subba Reddy and K. Praneeth, *Tetrahedron Lett.*, 2008, **49**(32), 4742.
16 X. D. Yang, X. H. Zeng, Y. H. Zhao, X. Q. Wang, Z. Q. Pan, L. Li and H. B. Zhang, *J. Comb. Chem.*, 2010, **12**(3), 307.
17 P. L. Warner Jr. and T. J. Bardos, *J. Med. Chem.*, 1970, **13**(3), 407.
18 A. R. Katritzky, C. Cai and S. K. Singh, *J. Org. Chem.*, 2006, **71**, 3375.
19 C. M. Bell, D. A. Kissounko, S. H. Gellman and S. S. Stahl, *Angew. Chem., Int. Ed.*, 2007, **46**, 761.
20 G. V. Boyd and R. L. Monteil, *J. Chem. Soc., Perkin Trans. 1*, 1978, 1338.
21 C. J. Cobley, M. van den Heuvel, A. Abbadi and J. G. de Vries, *Tetrahedron Lett.*, 2000, **41**, 2467.
22 S. Sharma, E. Park, J. Park and I. S. Kim, *Org. Lett.*, 2012, **14**(3), 906.
23 S. L. Jain, A. Modak and A. Bhaumik, *Green Chem.*, 2011, **13**, 586.
24 R. A. Sheldon, *Chem. Commun.*, 2008, 3352.